© 2013 The Chemical Society of Japan

Introduction of a Disulfide Bond as a Key Element of Acyclic Bis-Thiourea-Type Anion Receptors

Kentaro Tomita, Toshio Ishioka, and Akira Harata*

Department of Molecular and Material Sciences, Interdisciplinary Graduate School of Engineering Sciences, Kyushu University, Kasuga, Fukuoka 816-8580

Received September 30, 2013; E-mail: harata@mm.kyushu-u.ac.jp

This article shows that a difference in the building blocks of the molecular framework, C–C to S–S, results in a significant influence on its optical properties. Acyclic anion receptors, bis{2-[3-(substituted)thioureido]ethyl} disulfides were newly synthesized, and their optical properties in response to complex formation with an acetate ion were compared with those of a hexamethylene framework between two thioureido groups. Quantum chemical calculations suggested that receptors fold their molecular framework around disulfide because of the presence of the intramolecular hydrogen bonding between two *N*,*N*′-disubstituted thioureas. The complex of the receptor and the acetate ion with 1:1 stoichiometry consists of the coordination of two thioureido groups to the acetate via hydrogen bonds. This complex formation is accompanied by a dissociation of intramolecular hydrogen bonding and rotation of one side of the thioureido group. These circumstances of conformational changes in the molecular framework functioned by switching on and off the excimer fluorescence of the 1-pyrenylmethyl derivative.

Anionic species in living things, such as adenosine triphosphate, glutamic acid, and homovanillic acid, are important chemicals as an energy transporter,[1] a neurotansmitter,[2] and a tumor marker,[3] respectively. High-performance liquid chromatography is known as a conventional detection method for these anions.[4] This instrumental method is superior, in many aspects, though it is difficult to apply to in vivo and on-site analysis without any pretreatment procedures.

For these on-site applications, receptor molecules designed for anions, which consist of chromophores and ionophores, have attracted increasing attention.[5,6] These molecules can also be applied to a disposable checker for specific anion species and to a probe for confocal fluorescent microscopy.[7] For the successful spectrophotometric detection of ions in solutions, it is important to choose the molecular framework of the receptor from cyclic or acyclic. As for cation indicators, cyclic structures, such as crown ethers, are suitable for restricting the size of the recognition domain for the target ion.[8] The detection mechanism of this type of cation indicator is based on photoinduced electron transfer (PET),[9] twisted intramolecular charge transfer (TICT),[10] or exciplex formation.[11] Of these, PET is especially suitable for "off–on"-type fluorescent indicators because its quenching after excitation is inhibited by the coordination of the lone pair of electrons from oxygen or nitrogen on a cyclic framework to the targeted metal cation. Anion receptors with a cyclic framework are also reported;[12] however, the complex formation tends to be weak because they are led by hydrogen bondings. For higher binding constants of complex formation, precise positioning of ionophore groups is required to bind with the targeted anion because many kinds of anions consist of several oxygen atoms and show stereochemical effects. On the viewpoint of electron transfer, the binding of anions to ionophores, such as (thio)ureas and pyrroles, usually increases the reduction potential of the ionophore site and causes quenching of the fluorescence by PET from the ionophore-anion moiety to the singly occupied molecular orbital of the excited fluorophore. Therefore, the receptors are usually "on–off"-type fluorescent indicators.[13] Based on these circumstances of anion receptors, acyclic receptors have been developed as an alternative to cyclic receptors in terms of unique optical phenomena, such as excimer emission and Förster resonant energy transfer, in association with a drastic conformational change of the molecular framework promoted by the complex formation.[14–16]

In this paper, we have focused on acyclic anion receptors with two thioureylene groups on the terminal of the diethyl disulfide-based molecular framework (Scheme 1). These receptors showed unique changes in optical phenomena, such as hypsochromic effect and excimer emission, in association with complex formations with anions. We presumed that the disulfide moiety has a significant role in the behavior. Thus,

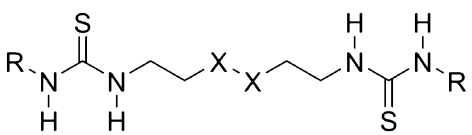

BPE : R= Phenyl , X= S
BBE : R= 4-Bromophenyl , X= S
BCE : R= 4-Chlorophenyl , X= S
BNE : R= 4-Nitrophenyl , X= S
BNH : R= 4-Nitrophenyl , X= CH_2
BNaE : R= 1-Naphthyl , X= S
BPyME: R= 1-Pyrenylmethyl, X= S

Scheme 1. Chemical formulas of anion receptors.

Published on the web December 12, 2013; doi:10.1246/bcsj.20130267

quantum chemical calculation was performed in order to discuss the conformation of the receptors. As a result, the disulfide bond arranges two thioureido groups close enough to form head-to-tail style intramolecular hydrogen bonding between the two thioureido groups. This intramolecular hydrogen bonding is dissociated by complex formation with various anions, such as singly charged anions (CH_3COO^-, $H_2PO_4^-$, and Cl^-) and oxalate ion. The conformational change in molecular framework was discussed experimentally by the suppression of the excimer fluorescence of the 1-pyrenylmethyl derivative.

Experimental

General. Cystamine dihydrochloride, phenyl, 4-bromophenyl, and 4-chlorophenyl isothiocyanates, 0.5 mol L^{-1} ethanol solution of potassium hydroxide, tetrabutylammonium (TBA) hydrogen sulfate, hexamethylenediamine, and organic solvents were purchased from Wako Pure Chemical Ind., Ltd. The 4-nitrophenyl and 1-naphthyl isothiocyanates were obtained from Tokyo Chemical Ind. Co., Ltd. Acetonitrile for high-performance liquid chromatography was purchased from Kishida Chemical Co., Ltd. TBA salts of dihydrogen phosphate, acetate, chloride, and nitrate were purchased from Sigma-Aldrich Co. LLC. Acetonitrile solutions containing 2.5×10^{-5} M of each receptor and 0–7 mM of TBA salts of each acid were prepared for spectrometry. The sample rested for 2 min before the measurement of UV–visible absorption spectra with a UV–visible spectrophotometer (UV-2550, Shimadzu Co., Ltd.). Stability constants between various combinations of the chosen receptor and one anion were obtained by the Benesi–Hildebrand plot. The stability constant of bis{2-[3-(4-nitrophenyl)thioureido]ethyl} disulfide, BNE, is obtained by nonlinear fitting of the absorption intensity at 367 nm. The fluorescence spectra of the pyrenylmethyl-substituted receptor, BPyME, in acetonitrile in the presence of TBA acetate were measured with a fluorospectrometer (FP-6600, JASCO Co., Ltd.). The sample of 5% butyl acetate–95% acetonitrile v/v solution contained 2.0×10^{-6} M of BPyME and 0–7 mM of TBA salt of acetate. Fluorescence spectra were measured after 8 min of storage in the spectrometer without photoirradiation. The excitation wavelength was 342 ± 5 nm, and the detected fluorescence resolution was 2 nm by setting the entrance and exit slit widths. The fluorescent intensities were integrated 4 times, with a scanning rate of 200 nm min^{-1}.

Synthesis of Receptors. Bis{2-[3-(substituted)thioureido]-ethyl} disulfides were synthesized from cystamine dihydrochloride and isothiocyanate derivatives. Cystamine dihydrochloride was dissolved in an ethanol solution containing 2.05 equivalents of potassium hydroxide and heated at 80 °C for 2 h. After the precipitated potassium chloride was removed, the solution was mixed with 2 equivalents of each isothiocyanate in ethanol and stirred for 2 h at 60 °C (after stirring the 1-naphthyl derivative at room temperature for 0.5 h). The obtained product was washed with ethanol, triturated with ether, and dried in vacuo. The completion of the reaction was confirmed with thin-layer chromatography before ^{1}H NMR and ^{13}C NMR measurements. Before the synthesis of BPyME, 1-pyrenylmethyl isothiocyanate was synthesized via dithiocarbamic acid tetramethylammonium salt.[17]

A receptor with a hexamethylene framework, 1,6-bis[3-(4-nitrophenyl)thioureido]hexane (BNH), was synthesized with a procedure similar to bis{2-[3-(substituted)thioureido]ethyl} disulfides from hexane-1,6-diamine and 4-nitrophenyl isothiocyanate in dichloromethane. The same washing procedure was done after the reaction.

Computational Method. For the optimization of the geometries of the receptors, density functional theory (DFT) calculation was performed with the Gaussian 09 suite of programs[18] at the B3LYP/6-311++G(d,p) level. The initial geometry was optimized with B3LYP/6-31G for BPE after semiempirical MO (PM6) calculations with MOPAC[19] (VERSION 6.03) through the Winmostar[20] interface.

To prepare the input file for the DFT calculation (B3LYP/6-311++G(d,p), gas phase) of BPE (tgggt)-2Ac complex, the ideal BPE (ttgtt) conformer containing two acetate ions near the thioureido groups was optimized with a DFT calculation (B3LYP/6-31++G(d,p), gas phase) after the MOPAC calculation.

Results and Discussion

Optimized Geometry of the Anion Receptors. The DFT calculation suggested the function of the receptors for nipping the anion. Two of the conformers of BPE optimized with the DFT calculation are shown in Figures 1A and 1C (other conformers with different geometry around thioureido groups

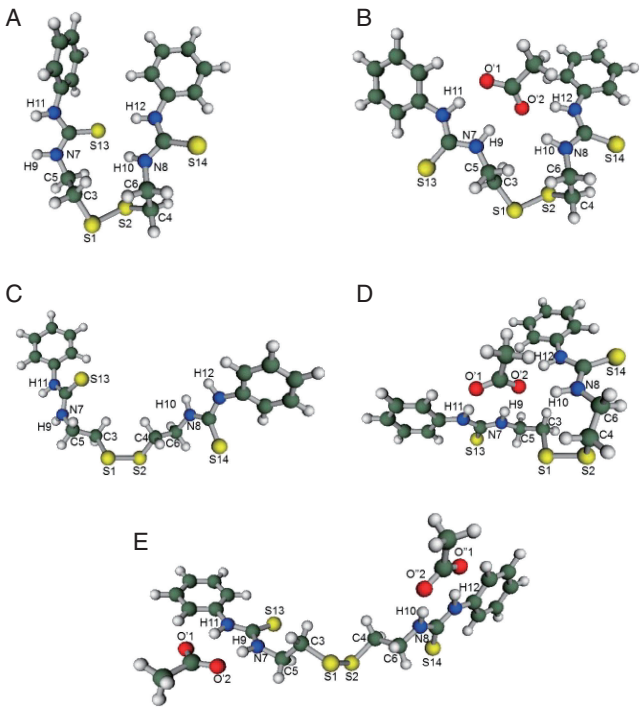

Figure 1. Structure of *cis*-thioureido conformers of BPE (A, C) and BPE-Ac complexes (B, D, E) calculated by DFT (B3LYP/6-311++G(d,p), gas phase). Orientation sequences of the diethyl disulfide framework of each conformer are tgggg (t: trans, g: gauche) (A, B), ttgtt (C), gtge′g (e: elipsed, prime: shift less than 20 degrees) (D), and tgggt (E) from C5 to C6 respectively. Conformers with *trans*-thioureido groups are shown in Figure S1 (Supporting Information).

Table 1. Calculated Dihedral Angles around Diethyl Disulfide Derived from Different Molecular Frameworks

Complexes (Conformation)	$q_{N7–C5–C3–S1}$ /degree	$q_{C5–C3–S1–S2}$ /degree	$q_{C3–S1–S2–C4}$ /degree	$q_{S1–S2–C4–C6}$ /degree	$q_{S2–C4–C6–N8}$ /degree
BPE(tgggg)	−174.12	68.26	93.44	−66.72	−60.94
BPE(tgggg)-Ac	169.14	−98.72	103.25	−73.05	−50.92
BPE(ttgtt)	−175.90	−170.28	88.08	−167.28	−179.48
BPE(gtge′g)-Ac	67.77	179.01	93.42	−107.80	74.05

Table 2. Zero-Point Corrected Relative Energies, Gibbs Free Energies, Enthalpy and Entropic Energy Changes at 298 K for Synthesized Receptors and Their Complexes with the Acetate Ion

Complexes (Conformation)[a)]	ΔE_{ZP} /kJ mol^{-1}	ΔG /kJ mol^{-1}	ΔH /kJ mol^{-1}	$T\Delta S$ /kJ mol^{-1}
BPE(tgggg)	0.00	0.00	0.00	0.00
BPE(ttgtt)	29.24	8.45	33.72	25.28
BPE(tgggg)-Ac	−226.84	−184.60	−222.70	−38.10
BPE(gtge′g)-Ac	−224.03	−186.03	−219.63	−33.60
BPE(tgggt)-2Ac	−205.15	−132.42	−197.94	−65.51
BPH(ttttt)	0.00	0.00	0.00	0.00
BPH(ttttt)-Ac	−168.49	−131.52	−165.85	−34.33
BPH(ttttt)-2Ac	−216.09	−137.34	−210.53	−73.20
BPH(ttgtt)	4.96	3.84	4.69	0.85
BPH(ttgg′g′)-Ac	−220.43	−164.83	−220.20	−55.37

a) Dihedral angles are shown in parentheses as g: gauche, t: trans, and e: eclipsed forms. Primes indicate the slight shift from each dihedral angle (less than 20 degrees).

Table 3. Charges on Each Oxygen Atom of Acetate and Total Charges on the Acetate Ion Calculated by Natural Bond Orbital Analysis (B3LYP/6-311++G(d,p), Gas Phase)

Complexes (Conformation)	Charges on each atom (*e*)		
	O1′	O2′	Total
BPE(tgggg)-Ac	−0.752	−0.847	−0.850
BPE(gtge′g)-Ac	−0.744	−0.852	−0.848
BPE(tgggt)-2Ac	−0.799	−0.773	−0.866
	−0.804[a)]	−0.766[a)]	−0.872[a)]
BPH(ttttt)-Ac	−0.799[a)]	−0.774[a)]	−0.865[a)]
BPH(ttttt)-2Ac	−0.804	−0.767	−0.873
	−0.802[a)]	−0.769[a)]	−0.873[a)]
BPH(ttgg′g′)-Ac	−0.744	−0.849	−0.850

a) These oxide atoms of the acetate ion are numbered with double prime mark in Figure 1E and Figure S2C (Supporting Information).

are summarized in Figure S1). The folded shape of the conformer (Figure 1A) had the intramolecular hydrogen bonding between two thioureido groups at both ends of diethyl disulfide with the orientation sequence trans–gauche–gauche–gauche–gauche (tgggg). The ggg conformation around disulfide bonding has been reported as the optimized conformation of the unit.[21,22] Figure 1B shows the optimized structure of the BPE-CH_3COO^- (BPE-Ac) complex. Two thioureido groups are coordinated to CH_3COO^- cooperatively. Accompanying this complex formation, the thioureido group at the left side is rotated +167° at the first S–C single bonding (Table 1). To determine the features of the disulfide bond, the optimized structures of BPH, which has a C–C single bond instead of a disulfide bond of BPE, and its acetate complex are also calculated. Table 2 shows the thermodynamic parameters for each conformer of BPE, BPH, and their complexes with acetate ions (The optimized structure of the BPE (gtge′g)-Ac complex is shown in Figure 1D). Enthalpies of acetate complexes without free thiourea groups are at almost the same level. On the other hand, the enthalpy of BPH(ttttt)-Ac (Figure S2B), which has fewer hydrogen bonds, is 55 kJ mol^{-1} smaller than BPH(ttgg′g′)-Ac (Figure S2E). These results indicate that the change in enthalpies can represent the sum of the strength of the hydrogen bonds. As for the change in free energies, the BPE(tgggg)-Ac complex is larger than those of the BPH-Ac complexes. This difference in the free energy means that the energy compensation caused by entropic loss is reduced by the presence of the disulfide bond. As the energy barrier of the rotation of the S–S bond is higher than that of the C–C bond,[21,23] it is known that the disulfide bonding has a stable 90° gauche-type dihedral angle. To investigate the stereochemical characteristic of the disulfide bond, we calculated the optimized structures and thermodynamic parameters (Table S1) of molecules, whose frameworks consist of *ortho*-, *meta*-, or *para*-benzene frameworks instead of disulfide bonding (refer to Figure S3). The molecule with the *ortho*-benzene framework is more stable than BPE, although entropic loss in their complexes with acetate was larger than that of BPE. These results confirm the uniqueness of the conformation around disulfide. For example, two side chains of BPE are in parallel order with suitable position for easier intramolecular hydrogen bonding. As for the two types of the BPE-acetate complex, two thioureido groups are close enough to form cooperative coordination to the acetate with the atomic ratio of O:H = 1:1, 1:3.

The restructuring of the hydrogen bonding is also confirmed in the charge density on the acetate ion calculated by natural bond orbital analysis (Table 3). Before the formation of the complex, BPE (tgggg) has a charge deviation between two side chains on the disulfide bond. The amount of the charge transfer was calculated to be 0.0126 *e* (*e*: elementary charge) from the left side to the right side in Figure 1A. After formation of the complex, part of the negative charge on the acetate was transported onto the receptor molecule. The BPE-Ac complex with conformations of trans–gauche–gauche–gauche–gauche (tgggg) and gauche–trans–gauche–elipsed–gauche (gtge′g) had the strongest charge transfer (−0.15 *e*) from the acetate to BPE. These features come originally from the unique dihedral angle and bond length of the disulfide bonding, keeping the molecular framework of BPE folded, reducing steric hindrance around the thioureido groups and enabling flexible complexion with reduced entropic loss.

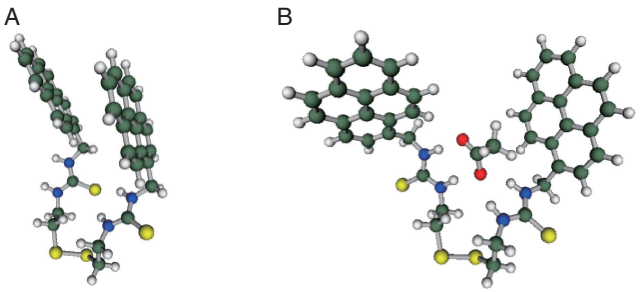

Figure 2. Structure of BPyME (A) and the BPyME-CH_3COO^- complex (B) calculated by DFT (B3LYP/6-311++G(d,p), gas-phase).

Morakot et al. reported an anion receptor with a glycol dialkyl ether-based molecular framework, and concluded that two thioureido groups within one receptor are suitable for dicarboxylate detection.[24] The binding energy of BPE for oxalate is also high because of the superior Lewis basicity of oxalate ions. The binding energies of BPE for various anionic species are also calculated (those optimized structures are shown in Figure S4) and summarized in Table S2. Oxoacids such as dihydrogenphosphate showed more entropic loss than did acetate and chloride ion. This feature results in the larger binding energy of BPE for acetate ion than for that of complexes with other oxoacids.

From Figures 1A and 1B, we see that BPE changes its conformational structure by switching the thioureido groups from the "head-to-tail" geometry to the "head-to-head" geometry across the acetate ion, and the distance between the two phenyl rings is elongated. Therefore, we hypothesized that this conformational change can be applied to design a function of switching off the excimer emission of the pyrenylmethyl derivative, BPyME. The addition of optical properties is a significant advantage over the cyclic molecule[25] consisting of three ethylene disulfide and three thioureido groups. The DFT calculations of BPyME and its complex with acetate ion were performed to obtain theoretical evidence for the function of switching off the excimer emission (Figures 2A and 2B). Two pyrenyl groups of BPyME are close because of the intramolecular hydrogen bonding of two thioureido groups. In contrast, two pyrenyl groups of the BPyME-Ac complex have a distance sufficient to avoid stacking. In this case, the thioureido group on the left side in Figure 2 was rotated, keeping the position of the methylene chains.

Measurement of the Complex with Intramolecular Excimer Quenching. Figure 3A shows the fluorescence spectra of BPyME in 5 vol % butyl acetate in acetonitrile upon the addition of tetrabutylammonium acetate salt. The fluorescent intensity of BPyME was totally decreased by the addition of acetate without large changes in the absorption spectra (Figure S5). The peak at 474 nm is assigned to the intramolecular excimer of BPyME (Verification of this peak whether it originates from intra- or intermolecular excimer is described in the Supporting Information. By the measurement of the excimer/monomer ratio vs. the concentration of BPyME in Figure S6, most of the emission at 474 nm is from intramolecular excimer.). The monomer fluorescence of the pyrenyl rings is also observed at 376 and 396 nm. A part of the monomer emission might originate from the photofragmentation products of the disulfide bond associated with the generation of the radical cation of the pyrenyl group.[26] This reaction was measured as the decrease of the ratio of fluorescence intensities at 474 and 376 nm (I_{474}/I_{376}) against the increase of the irradiation period (Figure S7). As I_{474} was proportional to exposuretime, the estimated initial values of I_{474}/I_{376} and the fraction of radiative decay resulting in excimer emission were 7.63 and 74% respectively. Details of the estimation are

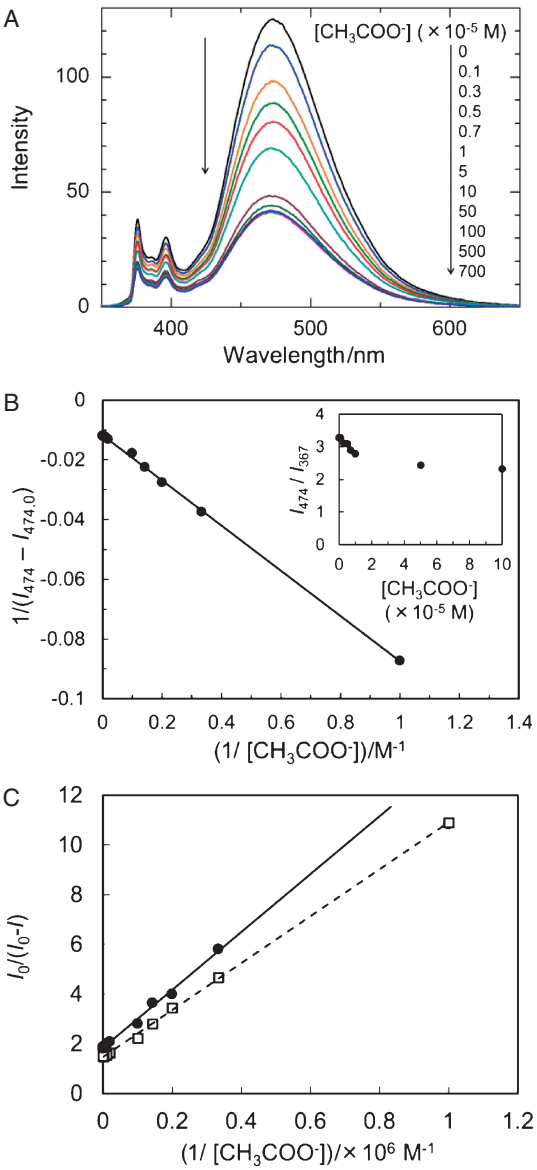

Figure 3. The fluorescence spectra (A) of BPyME in 5% butyl acetate–95% acetonitrile v/v solution in the presence of CH_3COO^- as tetrabutylammonium salt. The concentration of BPyME is 2×10^{-6} M. Benesi–Hildebrand plot for the peak of the excimer emission at 474 nm (B) showed the BPyME-CH_3COO^- complex with 1:1 stoichiometry. The plot of the intensity ratio at 474 and 376 nm vs. the concentration of acetate ion are inserted. (C) Linear plots of the quenching of fluorescence at 376 nm (●, solid line) and at 474 nm (□, dashed line).

in the Supporting Information. Assuming that 96% of monomer emission with 360 nm excitation originates from the opened form like Figure 1C, the estimated monomer emission measured with 342 nm excitation and 4 times integration consists of 57% of the photofragmentation products of the disulfide bonding. During 5 min of fluorescence measurement, the intensities of the excimer fluorescence at 474 nm were decreased $2.7 \pm 1.0\%$ regardless of the concentration of acetate ion (Figure S8). This result suggests that the addition of acetate itself does not induce nor accelerate the cleavage of disulfide.

The other part of the monomer emission observed suggests the presence of conformers with the trans form of the thioureido moiety or the opened form of the molecular framework represented by the conformer in Figure 1C. The excimer emission of molecules with two pyrenyl groups is influenced by the conformation of its molecular framework. For example, 1,*n*-bis(1-pyrenylcarboxy)alkanes show a different steric effect from that of 1,*n*-bis(1-pyrenyl)alkanes.[27,28] From the difference in conformation between methylene and ester, the lower rotational energy of the 1-pyrenylcarboxy group increases the frequency of the collision of chromophores to form dimer. The difference comes from the strong steric effect (intrachain H/H-repulsion of methylene) of 1,*n*-bis-(1-pyrenyl)alkanes. As for BPyME, the ratio of the quantum yield of excimer/monomer Φ'/Φ equals 6.81 calculated from the spectra with 342 nm excitation, and 18.1 with 360 nm excitation (the result of peak separation is shown in Figure S9). The small deviation comes from the difference in the rate of photofragmentation for each wavelength of excitation light. The Φ'/Φ of the BPyME with 342 nm excitation is still >1.86 times larger than that of 1,10-bis(1-pyrenylcarboxy)decane in methylcyclohexane at 20 °C. This result suggests that the small difference in the rotational energy of each bond[21,29] largely influences the average conformation of sequentially changing conformers. The receptor reported by Dahan et al.[15] also has two (1-pyrenylmethyl)thiourea groups at terminals of the linear molecular framework, though BPyME has a larger Φ'/Φ. This difference also suggests that the combination of disulfide between two thiourea groups is preferable for the collision of chromophores resulting in intramolecular excimer formation.

The Benesi–Hildebrand plot[30] (B–H plot) for the fluorescence spectra of BPyME-CH_3COO^- is shown in Figure 3B. Linear relation against inverse of the *n*-th power of the concentration of guest molecule means the host–guest association reaction is 1:*n* stoichiometry. Therefore, the peak at 474 nm of BPyME, which mainly consisted of the intramolecular excimer emission, was quenched in association with the formation of the complex with the ratio of receptor:anion = 1:1. The ratio of the intensities at 474 nm over 376 nm (I_{474}/I_{376}) was plotted versus the concentration of acetate ion is inserted in Figure 3B (inserted). Decrease in the ratio suggests the binding of acetate ion associates excimer dissociation, though the exciplex emission of the group of 3-(1-pyrenylmethyl)-thioureido-acetate complexes rises at 472 nm in parallel with the excimer quenching. The value of $I_{474}/I_{376} > 2$ corresponds to the higher binding constant of BPyME and acetate ion ($1.5 \times 10^5\,M^{-1}$) than that of 3-pyrenylmethyl-1-methyl thiourea ($5.7 \times 10^3\,M^{-1}$).[31]

The Stern–Volmer plot for the two peaks (Figure S10) showed a significant downward bend. Under this circumstance, the Hindered Access Model can explain the result.[32] In this model, there are two fluorophores with different accessbility to the quencher. The quenching is linearized with the equation below:

$$\frac{I_0}{(I_0 - I)} = \frac{1}{f\,K_{SV}}\frac{1}{[Q]} + \frac{1}{f} \quad (1)$$

where I_0 and I are the fluorescent intensities obtained from the BPyME and its complex with [Q] M of acetate ion. K_{SV} is the Stern–Volmer constant, and f is the fraction of the accessible fluorophore. Values of K_{SV} and f obtained from Figure 3C were $1.57 \times 10^5\,M^{-1}$ and 0.55, respectively, for monomer emissions and $1.52 \times 10^5\,M^{-1}$ and 0.69, respectively, for excimer emissions. In spite of the homogeneous solution of BPyME, the half of the fluorophore for the monomer emission is hindered from the quencher. Therefore the f value seems to represent the BPyME-acetate complex that contains two fluorophores (one is accessible and the other is inaccessible) per one acetate ion. The molecular orbitals calculated with DFT-B3LYP/6-311++G(d,p) are helpful for discussing the hindered fluorophore of BPyME-acetate complex. Before complexation, molecular orbitals on either pyrenyl ring can be considered independent of the other pyrenyl ring (Figure S11).

After formation of the complex with acetate ion, this circumstance is not changed, suggesting that another pyrenyl ring on the other side can behave as a hindered fluorophore during the exciplex formation. In the case of the excimer emission, all fluorophores are accessible. Therefore the fraction f was higher than that of the monomer emission.

From the fluorescence experiment described above, the conformational change in the complex formation of the acetate ion and BPyME is suggested as Scheme 2. BPyME forms the 1:1 complex with acetate ion accompanied by the rotation of a 1-pyrenylmethylthioureirene group. This conformational change induces dissociation of intramolecular excimer. However most of the monomer fluorescence is suppresed by the exciplex formation. To verify the "disulfide bonding assisted" stable 1:1 complex formation and the function of anion recognition by the rotation of end group, UV–visible absorption spectra of 4-nitrophenyl-substituted receptors with diethyl disulfide or hexamethylene framework were measured.

Experimental Validation of the Role of the Disulfide Bonding. UV–visible absorption spectra of BNE in the presence of CH_3COO^- as TBA salts are shown in Figure 4A. Because of the electron-withdrawing nitro substitution, a strong absorption of the intramolecular charge transfer (ICT) at 338.5 nm showed a clear peak shift to 367 nm via the appearance of a suspending peak at 352.5 nm. The B–H plots for absorption spectra[33] shown in Figure 4B indicate that the complexation was 1:1 for dilute acetate and 1:*n* ($n > 1$) for concentrated acetate. The peak shift means that the donor ability of the thiourea moiety is enhanced by the acetate ion.[34] The stability constant for the 1:1 complex of BNE with the acetate ion was calculated as $2.5 \times 10^6\,M^{-1}$ by the fitting procedure (Figure S12) $0–7 \times 10^{-5}$ M. This stability constant is 5 times larger than that of a monosubstituted thiourea derivative,[35] 1-methyl-3-(4-nitrophenyl)thiourea, $5.0 \times 10^5\,M^{-1}$. This difference indicates that two ionophores of BNE orient cooperatively

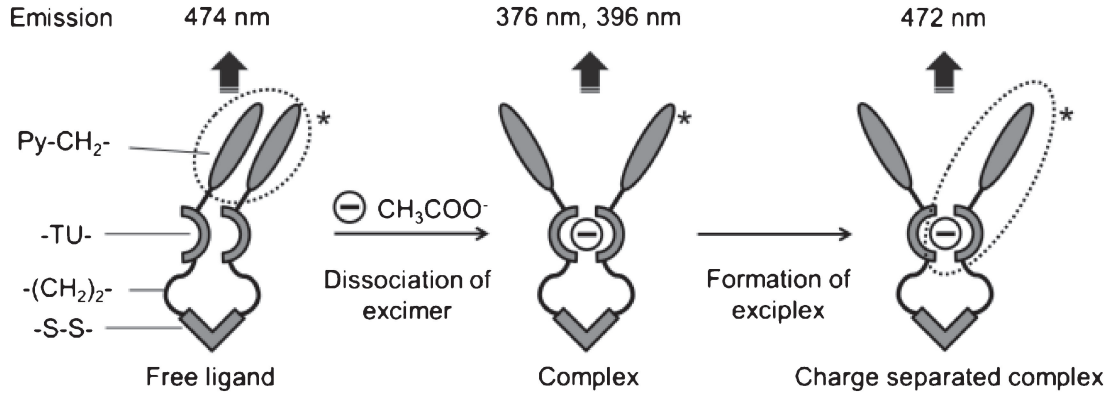

Scheme 2. The pathway of radiative-relaxation surrounding the complex formation of BPyME and acetate. Asterisks represent excited groups. The peak wavelengths of fluorescence corresponding to each excited group are denoted at the top of illustrations.

for an acetate ion. This difference corresponds to the difference in free energy obtained by DFT calculations in the gas phase, $\Delta G = -242.75\,\mathrm{kJ\,mol^{-1}}$ for the BNE-acetate complex and $\Delta G = -168.98\,\mathrm{kJ\,mol^{-1}}$ for the 1-methyl-3-(4-nitrophenyl)-thiourea-acetate complex. We note here that deprotonation of the 4-nitrophenyl-substituted thiourea part of BNE was not observed. It is known that 1-methoxyethyl-3-(4-nitrophenyl)-thiourea causes a new peak around 460 nm in the presence of excess acetate in acetonitrile.[36] However, in the case of BNE, the decrease of the absorbance at 367 nm and the increase of a new peak at 460 nm were not measured in the presence of excess acetate ion (Figure 4A). This result indicates that the deprotonation of thioureido group was not caused by the high stability of the BNE-Ac complex compared to the stability of the $(CH_3COO)_2H^-$ complex,[37] $(9.7 \pm 0.2) \times 10^3\,\mathrm{M^{-1}}$ in acetonitrile. Stability for deprotonation was also verified with NMR measurement in Figure S13.

The B–H plots of BNH are shown in Figure 4B for 1:1 complex and in Figure 4C for 1:2 complex (receptor:acetate). The binding constant of 1:1 complex can be calculated as $2.0 \times 10^6\,\mathrm{M^{-1}}$ from the absorbance change at 362 nm upon the addition of CH_3COO^- (details of the fitting are shown in Figure S12), although B–H plots showed the 1:2 complex formation. This result means each side of two ionophores groups in BNH binds to acetate independently. The difference in the stoichiometry of BNE and BNH acetate complexes suggests that the folded structure of disulfide bonding clearly supports the stability of 1:1 complex of acyclic receptor molecule and acetate. Quantum chemical calculations for BPE and BPH, summarized in Table 2, support this difference between diethyl disulfide and hexamethylene frameworks: The binding energy of 1:1 complex of BPE and acetate is $53\,\mathrm{kJ\,mol^{-1}}$ higher than that of the 1:2 complex, while the corresponding difference of the BPH-acetate complexes is $27\,\mathrm{kJ\,mol^{-1}}$.

The conformational change around terminal groups induced by the complex formation was discussed through the comparison of the absorption peak wavelength of ICT in BNE and BNH in the presence of acetate ion (Figure 5A). The peak wavelength of ICT in BNE shifted ca. 3 nm to blue relative to ICT in BNH. This hypsochromic effect agrees with the folded structure of BNE. The interaction between two 4-nitrophenylene-1-thiourea groups, whose dipole moments of the ICT state are parallel ordered, leads to the increase of the excitation energy.[38] The computational calculations on BNE and BNH shown in Figures 5B and 5C support the idea of a difference in conformation of the average structure. The free energy of BNE changes by $-5.70\,\mathrm{kJ\,mol^{-1}}$ with the folding reaction from the trans–gauche–gauche–trans–trans (tggtt) form to the tgggg form, while the change in the free energy of the folding reaction of BNH from the ttttt form to the same orientation sequence (tgggg) is $11.65\,\mathrm{kJ\,mol^{-1}}$. From the difference of the calculated ΔH of the folding reaction ($1.52\,\mathrm{kJ\,mol^{-1}}$ for BNH $> 0 >$ $-26.35\,\mathrm{kJ\,mol^{-1}}$ for BNE), the disulfide bond is working as the key element for the formation of intramolecular hydrogen bonding.

Complex Formation of Receptors with Various Anions. The stability constants, K_s, are summarized in Table 4 for each receptor, such as BPE, with CH_3COO^-, $H_2PO_4^-$, Cl^-, HSO_4^-, and NO_3^-. Those values were obtained from the B–H plot done on each absorption spectrum (Figures 4B and S14–S19). Comparison of the K_s of BNE and BNH reveals that BNE tends to form a more stable complex with planar anions, in this case CH_3COO^- and NO_3^-, than that of BNH. On the other hand, the K_s of nitro-substituted receptors and tetrahedral anions, $H_2PO_4^-$ and HSO_4^-, were decreased by the introduction of disulfide bonding. This is because the disulfide bonding at the center of the molecular framework supports cooperative coordination with two ionophores at both ends while it restricts possible conformations suitable for tetrahedral anions which have more binding sites than planar anions.

Stability constants corresponding 1:1 to the complexes of disulfide-based receptor and each anion in Table 4 show that the substitution of functional groups on the phenylene ring can control the selectivity for anions. The more electron-withdrawing the substitution group is, the more selective the receptor is for acetate ion, while it becomes less selective for dihydrogen phosphate ion. This substitutional effect can be described by the Hammett equation:[40]

$$\log\left(\frac{K_{s,R}}{K_{s,H}}\right) = \rho\sigma \tag{2}$$

where indices R and H represent the element on 4-substitution to each receptor and ρ is the constant for the specific complex formation reaction. When ρ equals 1, the reaction equilibrium

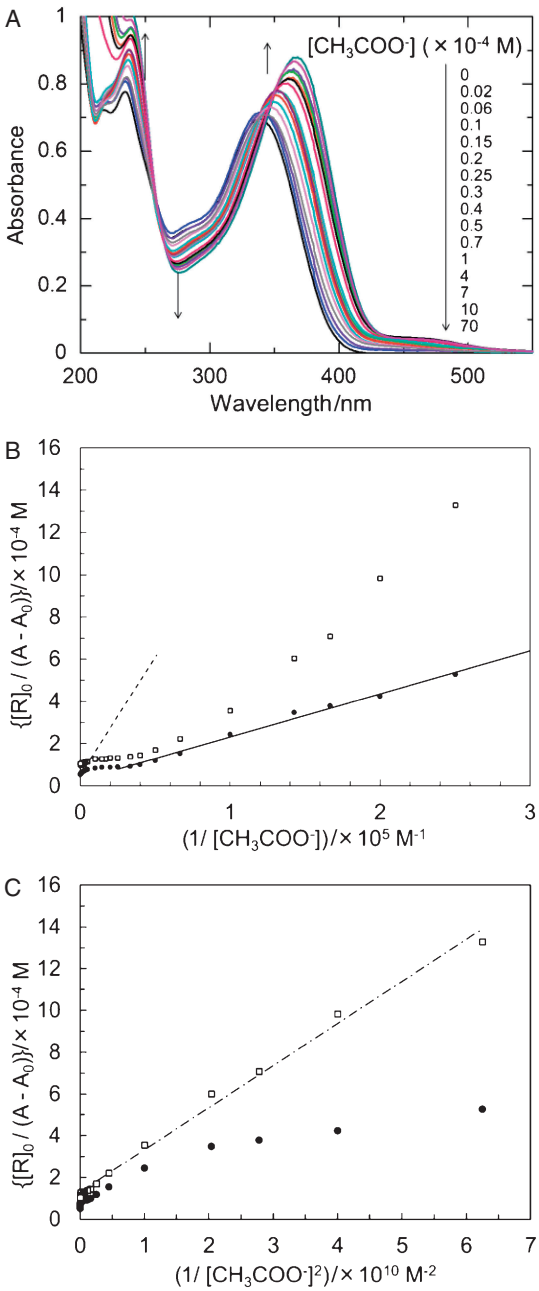

Figure 4. UV–visible absorption spectrum of BNE with acetate in acetonitrile (A) and its Benesi–Hildebrand plot (B, C). Three linear lines are mathematically fit to the complexes with the BNE:CH_3COO^- = 1:1 (solid line), BNE-CH_3COO^-:CH_3COO^- = 1:1 (broken line, the entire stoichiometry is 1:2) and 1:2 (dashed-dotted line) stoichiometry. The theoretical equation is described in Ref. 33.

for the selected substitution is equal to the reaction of the ionization of benzoic acid. The symbol σ is the substituent constant. Figure 6 shows the plot of $\log(K_{s,R}/K_{s,H})$ vs. σ of receptors for each acid. Slopes ρ for each anion were 3.4 (CH_3COO^-) > 1.7 (NO_3^-), 1.5 (HSO_4^-), and 1.3 (Cl^-) > 0 > −1.1 ($H_2PO_4^-$). Slope ρ for the plot shows that the affinity of the host to the guest has a relation between each anion's hardness and the electron density of the hydrogen atoms on the thiourea groups.

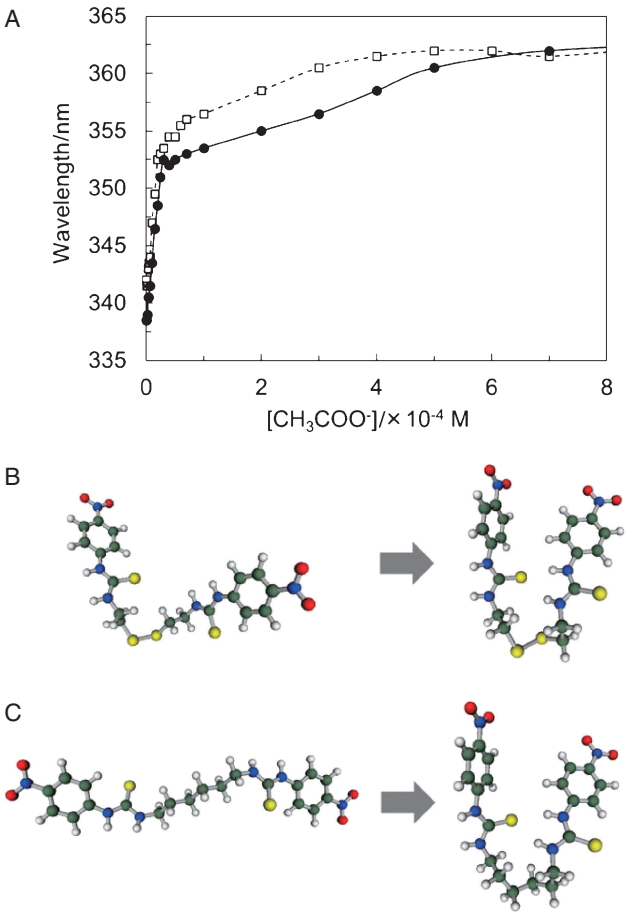

Figure 5. The peak position of the intramolecular charge transfer absorption band of 4-nitrophenyl derivatives, BNE (●, solid line) and BNH (□, dashed line) with various concentrations of acetate ion as a TBA salt in acetonitrile (A); changes in B3LYP-optimized structures from the unfolded form (tggtt, left side) to the folded form (tgggt, right side) of BNE (B), and from the unfolded form (ttttt, left side) to the folded form (tgggt, right side) of BNH (C).

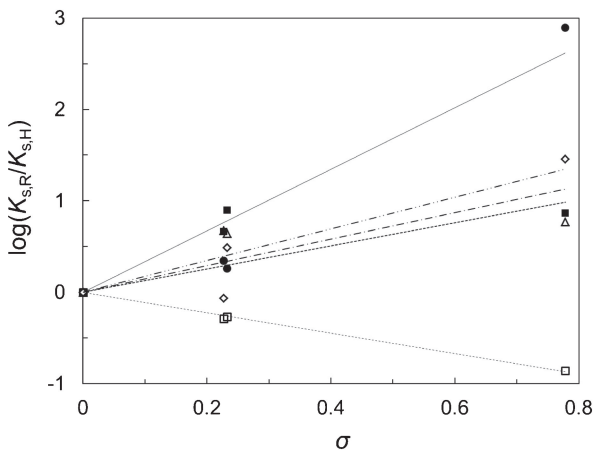

Figure 6. Plot of $\log(K_{s,R}/K_{s,H})$ vs. σ for CH_3COO^- (solid circle), NO_3^- (unshaded diamond), HSO_4^- (solid square), Cl^- (unshaded triangle), and $H_2PO_4^-$ (unshaded square) in acetonitrile at room temperature.

Table 4. Stability Constants, K_s (M^{-1}), of Receptors with a Variety of Anionic Guests as TBA Salts at 298 K in Acetonitrile

Receptor	Substitution on thiourea	Binding constant/M^{-1}					Hammett constant[f] σ
		CH_3COO^-	$H_2PO_4^-$	Cl^-	HSO_4^-	NO_3^-	
BPE	phenyl	3.2×10^3	1.8×10^4	3.4×10^3	1.9×10^2	2.9×10^1	0
BCE	4-chlorophenylene	7.1×10^3	9.3×10^3	1.6×10^4 (4.5×10^3)[a]	8.8×10^2 (3.7×10^2)[a]	2.5×10^1	0.227
BBE	4-bromophenylene	6.5×10^3	9.7×10^3	1.5×10^4 (3.5×10^3)[a]	1.5×10^3 (4.5×10^2)[a]	8.9×10^1	0.232
BNE	4-nitrophenylene	2.5×10^6[g] (2.3×10^3)[a]	2.5×10^3	2.0×10^4 (1.4×10^3)[a]	1.4×10^3[c]	8.3×10^2	0.778
BNH	4-nitrophenylene	2.0×10^6[g] (6.5×10^9)[b]	2.2×10^4	2.8×10^4	2.2×10^3	4.5×10^2	0.778
BNaE	1-naphthyl	3.1×10^4	1.2×10^4	8.2×10^2	2.9×10^1	5.6	—
BPyME	1-pyrenylmethyl	1.6×10^5[d], 1.5×10^5[e]	3.3×10^4[d], (4.8×10^9)[b,e]	2.0×10^3[d], 2.8×10^3[e]	4.2×10^2[e]	7.3×10^2[e]	—

a) The 2nd binding constants of the 1:2 complex (M^{-1}) via stable 1:1 complexes. b) The binding constants of the receptor:anion = 1:2 complex (M^{-2}) directly formed. c) This value was reported in a previous work.[39] d) Obtained with the peak of the monomer emission at 376 nm in fluorescence spectra. e) Obtained with the peak of the excimer emission at 474 nm in fluorescence spectra. f) Ref. 40. g) Calculated by the fitting procedure for absorbance (Figure S12).

It is known that ρ is >0 in many cases.[41] Therefore, a negative slope for dihydrogen phosphate ion seems to be strange. However, the 1:2 complex formation of $H_2PO_4^-$ and BPyME, which has the most electron-donating group on thiourea groups among receptor molecules in this report, supports that $H_2PO_4^-$ tends to form a stronger complex by the substitution of electron-donating groups (Figure S19). The reason is unclear, though we hypothesize that (1) the amount of entropic loss containing the reorganization of solvent molecules is lowered by the electron-donating substitution in the case of the complex formation of $H_2PO_4^-$ and thiourea group; (2) the intramolecular hydrogen bonding of the receptor with the electron-withdrawing substitution is strong enough to inhibit the complex formation with the tetrahedral anions, especially $H_2PO_4^-$, namely the spatial selectivity for planar anions is enhanced. Further investigation is required to clarify these hypotheses for the relationship between ρ and the level of the spatial selectivity.

Conformational changes induced by anion recognition are summarized in Scheme 3. By the presence of intramolecular hydrogen bonding, the distance between both terminal groups of free receptor molecule is small enough to have an interaction. After the addition of acetate, a side of ionophores rotates to form the stable 1:1 complex. Excess amount of acetate causes the formation of the 1:2 complex. The entire host–guest reaction consists of two 1:1 complexation reactions: pathway (i). In the case that the ionophores and anion have strong interaction, such as the combination of BPyME and $H_2PO_4^-$, the direct 1:2 complex formation occurs: pathway (ii). The ionophore groups of the receptor with the hexamethylene framework tend to behave as independent binding sites.

Conclusion

The conformational change of anion receptors consisted of two thioureido groups on the terminals of diethyl disulfide as the molecular framework was discussed theoretically and experimentally. From the results of DFT calculation, the disulfide bond works as a folding point. Under the circumstance, the formation of the intramolecular hydrogen bonding between two thioureido groups was suggested to explain the tendency for a folded molecular framework of free receptors. The intramolecular hydrogen bonding and the configuration of the disulfide bond reduce the entropic loss in complex formation with anions. From the experimental results, the stable 1:1 complex formation with anion species is suggested as if receptors work as molecular tweezers for anions. The conformational change in the framework was clearly observed from static fluorescence of a 1-pyrenylmethyl derivative. In comparing the experimental result of the receptors with the diethyl disulfide framework and the hexamethylene framework, the receptor with the disulfide bond showed a clear blue shift of the peak position of the intramolecular charge transfer of the 4-nitrophenyl derivative. DFT calculations for changes in the free energies of the folding reaction suggested that the valid blue shift in UV–visible absorption spectra is related to the presence of intramolecular hydrogen bonds generated by the substitution effect of the disulfide bond.

This report features the property of disulfide as a building block of a receptor molecule for anions. The other building blocks might be examined with the method we used; analyzing dimerization of pyrene by calculation and fluorescence experiments will make it easier to design and control functional molecules.

This work was partly supported by a JSPS Grant-in-Aid for Scientific Research (C) No. 23550098, and a grant from the Global Centre of Excellence in Novel Carbon Resource Sciences, Kyushu University.

Supporting Information

Characterizations of compounds synthesized, figures, and tables labeled with "S" in the text describing the B3LYP optimized conformations of BPE, for example, are in other material. This material is available free of charge on the Web at: http://www.csj.jp/journals/bcsj/.

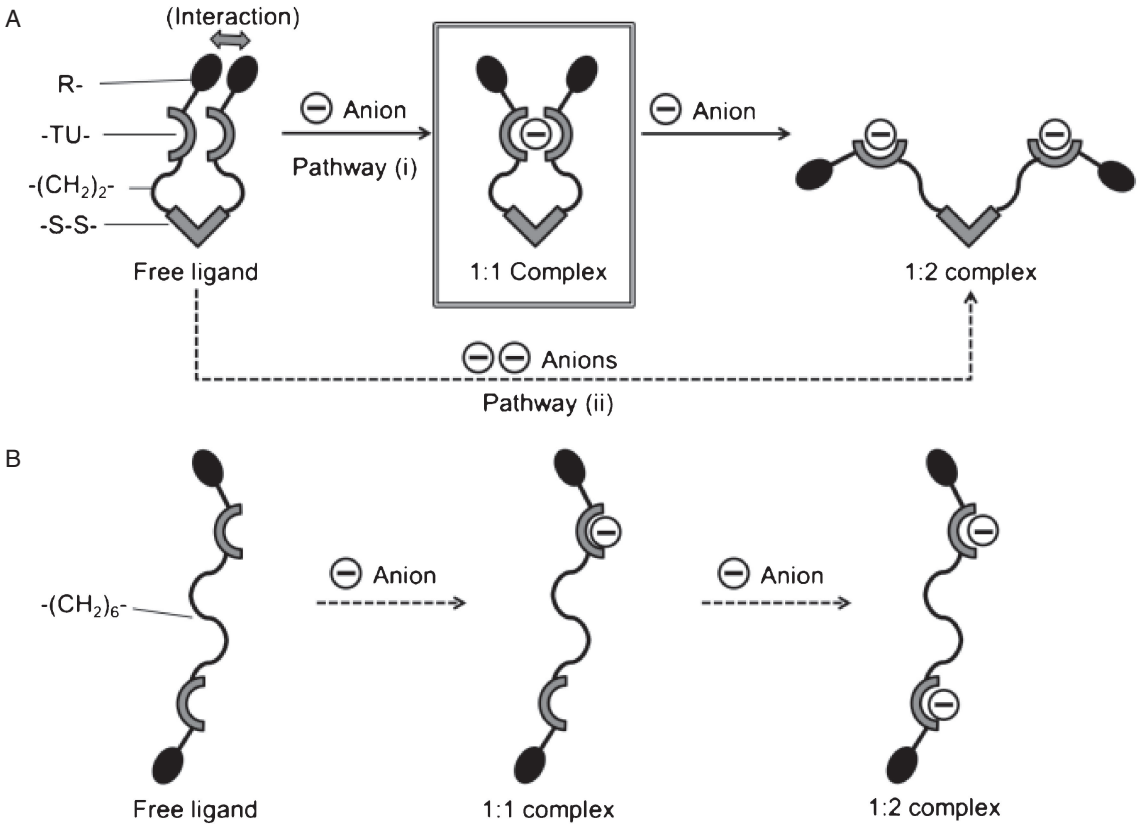

Scheme 3. Pathways for the complex formation of disulfide-based receptors with various anions: the phased complex formation via the stable 1:1 complex (pathway (i), A) and the complex formation with isolated-terminal ionophores, which can be observed as receptor:anion = 1:2 stoichiometry by B–H plot analysis (pathway (ii), A). The pathway of the complex with hexamethylene framework is described as similar pathway (ii) (B).

References

1 E. Pebay-Peyroula, C. Dahout-Gonzalez, R. Kahn, V. Trézéguet, G. J.-M. Lauquin, G. Brandolin, *Nature* **2003**, *426*, 39.

2 V. Parpura, T. A. Basarsky, F. Liu, K. Jeftinija, S. Jeftinija, P. G. Haydon, *Nature* **1994**, *369*, 744.

3 V. Strenger, R. Kerbl, H. J. Dornbusch, R. Ladenstein, P. F. Ambros, I. M. Ambros, C. Urban, *Pediatr. Blood Cancer* **2007**, *48*, 504.

4 G. Grossi, A. M. Bargossi, C. Lucarelli, R. Paradisi, C. Sprovieri, G. Sprovieri, *J. Chromatogr., A* **1991**, *541*, 273.

5 T. Gunnlaugsson, M. Glynn, G. M. Tocci, P. E. Kruger, F. M. Pfeffer, *Coord. Chem. Rev.* **2006**, *250*, 3094.

6 I. Ohshiro, M. Ikegami, Y. Shinohara, Y. Nishimura, T. Arai, *Bull. Chem. Soc. Jpn.* **2007**, *80*, 747.

7 Y. Kurishita, T. Kohira, A. Ojida, I. Hamachi, *J. Am. Chem. Soc.* **2010**, *132*, 13290.

8 T. Nabeshima, *Bull. Chem. Soc. Jpn.* **2010**, *83*, 969.

9 T. Gunnlaugsson, B. Bichell, C. Nolan, *Tetrahedron Lett.* **2002**, *43*, 4989.

10 G. E. Collins, L.-S. Choi, J. H. Callahan, *J. Am. Chem. Soc.* **1998**, *120*, 1474.

11 S. Nishizawa, M. Watanabe, T. Uchida, N. Teramae, *J. Chem. Soc., Perkin Trans. 2* **1999**, 141.

12 S. Otto, S. Kubik, *J. Am. Chem. Soc.* **2003**, *125*, 7804.

13 T. Gunnlaugsson, A. P. Davis, G. M. Hussey, J. Tierney, M. Glynn, *Org. Biomol. Chem.* **2004**, *2*, 1856.

14 S. Kondo, S.-i. Nakajima, M. Unno, *Bull. Chem. Soc. Jpn.* **2012**, *85*, 698.

15 A. Dahan, T. Ashkenazi, V. Kuznetsov, S. Makievski, E. Drug, L. Fadeev, M. Bramson, S. Schokoroy, E. Rozenshine-Kemelmakher, M. Gozin, *J. Org. Chem.* **2007**, *72*, 2289.

16 H. J. Kim, S. Y. Park, S. Yoon, J. S. Kim, *Tetrahedron* **2008**, *64*, 1294.

17 R. Wong, S. J. Dolman, *J. Org. Chem.* **2007**, *72*, 3969.

18 M. J. Frisch, G. W. Trucks, H. B. Schlegel, G. E. Scuseria, M. A. Robb, J. R. Cheeseman, G. Scalmani, V. Barone, B. Mennucci, G. A. Petersson, H. Nakatsuji, M. Caricato, X. Li, H. P. Hratchian, A. F. Izmaylov, J. Bloino, G. Zheng, J. L. Sonnenberg, M. Hada, M. Ehara, K. Toyota, R. Fukuda, J. Hasegawa, M. Ishida, T. Nakajima, Y. Honda, O. Kitao, H. Nakai, T. Vreven, J. A. Montgomery, Jr., J. E. Peralta, F. Ogliaro, M. Bearpark, J. J. Heyd, E. Brothers, K. N. Kudin, V. N. Staroverov, R. Kobayashi, J. Normand, K. Raghavachari, A. Rendell, J. C. Burant, S. S. Iyengar, J. Tomasi, M. Cossi, N. Rega, J. M. Millam, M. Klene, J. E. Knox, J. B. Cross, V. Bakken, C. Adamo, J. Jaramillo, R. Gomperts, R. E. Stratmann, O. Yazyev, A. J. Austin, R. Cammi, C. Pomelli, J. W. Ochterski, R. L. Martin, K. Morokuma, V. G. Zakrzewski, G. A. Voth, P. Salvador, J. J. Dannenberg, S. Dapprich, A. D. Daniels, Ö. Farkas, J. B. Foresman, J. V. Ortiz, J. Cioslowski, D. J. Fox, *Gaussian 09 (Revision C.01)*, Gaussian, Inc., Wallingford CT, **2009**.

19 J. J. P. Stewart, *MOPAC 6.0*, Frank J. Seiler Research Lab, U. S. Air Force Academy, CO, **1990**.

20 N. Senda, *Winmostar, version 4.010* (URL: http://winmostar.com/).

21 W. L. Jorgensen, D. S. Maxwell, J. Tirado-Rives, *J. Am. Chem. Soc.* **1996**, *118*, 11225.
22 K. R. Ackermann, J. Koster, S. Schlücker, *Chem. Phys.* **2009**, *355*, 81.
23 P. Vansteenkiste, V. Van Speybroeck, E. Pauwels, M. Waroquier, *Chem. Phys.* **2005**, *314*, 109.
24 N. Morakot, W. Rakrai, S. Keawwangchai, C. Kaewtong, B. Wanno, *J. Mol. Model.* **2010**, *16*, 129.
25 Y. Chen, X. Pan, H. Yan, N. Tan, *Phys. Chem. Chem. Phys.* **2011**, *13*, 7384.
26 M. You, Z. Zhu, H. Liu, B. Gulbakan, D. Han, R. Wang, K. R. Williams, W. Tan, *ACS Appl. Mater. Interfaces* **2010**, *2*, 3601.
27 K. A. Zachariasse, A. L. Maçanita, W. Kühnle, *J. Phys. Chem. B* **1999**, *103*, 9356.
28 T. Kanaya, K. Goshiki, M. Yamamoto, Y. Nishijima, *J. Am. Chem. Soc.* **1982**, *104*, 3580.
29 M. L. P. Price, D. Ostrovsky, W. L. Jorgensen, *J. Comput. Chem.* **2001**, *22*, 1340.
30 A. Banerjee, A. Sahana, S. Guha, S. Lohar, I. Hauli, S. K. Mukhopadhyay, J. S. Matalobos, D. Das, *Inorg. Chem.* **2012**, *51*, 5699.
31 S. Nishizawa, H. Kaneda, T. Uchida, N. Teramae, *J. Chem. Soc., Perkin Trans. 2* **1998**, 2325.
32 S. S. Lehrer, *Biochemistry* **1971**, *10*, 3254.
33 H. A. Benesi, J. H. Hildebrand, *J. Am. Chem. Soc.* **1949**, *71*, 2703.
34 A. Oehlke, A. A. Auer, K. Schreiter, K. Hofmann, F. Riedel, S. Spange, *J. Org. Chem.* **2009**, *74*, 3316.
35 S. Nishizawa, R. Kato, T. Hayashita, N. Teramae, *Anal. Sci.* **1998**, *14*, 595.
36 C. Pérez-Casas, A. K. Yatsimirsky, *J. Org. Chem.* **2008**, *73*, 2275.
37 J. Zielińska, M. Makowski, K. Maj, A. Liwo, L. Chmurzyński, *Anal. Chim. Acta* **1999**, *401*, 317.
38 S. Okada, H. Segawa, *J. Am. Chem. Soc.* **2003**, *125*, 2792.
39 K. Tomita, T. Ishioka, A. Harata, *Anal. Sci.* **2012**, *28*, 1139.
40 L. P. Hammett, *J. Am. Chem. Soc.* **1937**, *59*, 96.
41 N. Busschaert, S. J. Bradberry, M. Wenzel, C. J. E. Haynes, J. R. Hiscock, I. L. Kirby, L. E. Karagiannidis, S. J. Moore, N. J. Wells, J. Herniman, G. J. Langley, P. N. Horton, M. E. Light, I. Marques, P. J. Costa, V. Félix, J. G. Frey, P. A. Gale, *Chem. Sci.* **2013**, *4*, 3036.